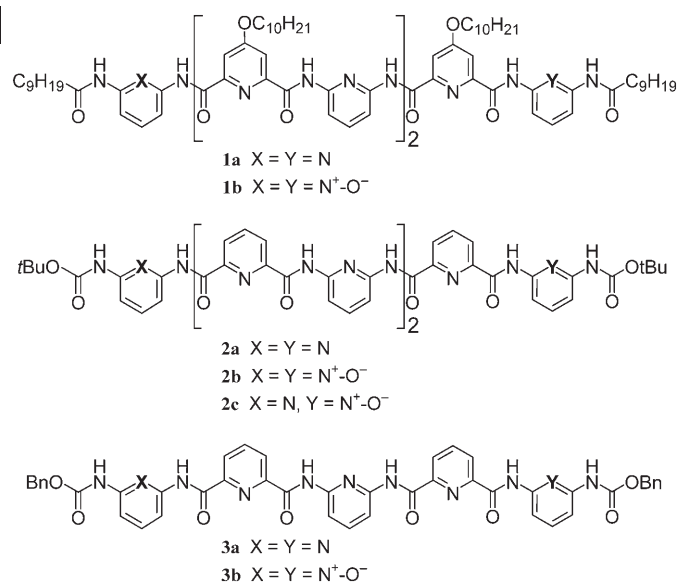


Cross-Hybridization of Pyridinedicarboxamide Helical Strands and Their *N*-Oxides**

Chuanlang Zhan, Jean-Michel Léger, and Ivan Huc*

Chemists have exploited the ability of nucleic acids to form sequence-selective double-stranded hybrids and have turned it into an incredibly powerful tool to direct chemical synthesis^[1] and to create well-defined discrete nanoarchitectures and two-dimensional patterns.^[2] Non-natural double-stranded molecules held together by noncovalent interactions which mimic nucleic acid hybridization^[3] may potentially be useful in a similar way. For example, hydrogen-bonded duplexes based on linear oligoamide strands have recently been used to template cross-olefin metathesis.^[4] Such applications require the hybridization of two *different* strands to form a cross-hybrid so that each strand can selectively bring a given functionality or a given structural unit to the duplex. In DNA, this is expressed by the fact that the basic level of complementarity—canonical A/T and G/C base pairing—is indeed heterologous and not homologous. However, most synthetic oligomers that hybridize into double-stranded structures reported to date are homodimers, including most of the numerous helicates,^[5] hydrogen-bonded linear tapes^[6–10] and helices,^[11] as well as the aromatic oligoamides (AOAs) derived from 2,6-diaminopyridine and 2,6-pyridinedicarboxylic acid that we have been studying.^[12,13] There are only a few examples of heterodimerized oligomeric strands that form helicates^[14] and hydrogen-bonded structures,^[4,15,16] as well as of hybrids based on the assembly of electron-poor and electron-rich aromatic compounds,^[17] but among these, less than a handful (two to our knowledge)^[14,16] possess a well-characterized structure. Herein, we describe our discovery of a cross-hybridization between double helices formed by AOAs and their *N*-oxide derivatives.

In solution, oligomers such as **1a**, **2a**, and **3a** (Scheme 1) form single helices^[18] that can extend like springs and intertwine into double-helical homodimers.^[12,19] The single



Scheme 1. Oligomers studied. Bn = benzyl.

and double helices are in slow exchange on the NMR timescale, thus giving rise to two sets of signals for heptamer **1a** (Figure 1a) and for heptamer **2a** (Figure 2a). The

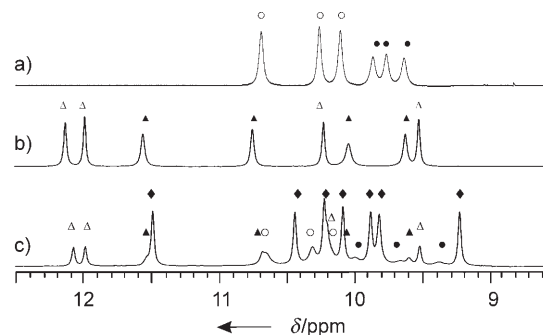


Figure 1. Partial 400 MHz ¹H NMR spectra at 25 °C showing the amide resonances of: a) **1a** (8 mm), b) **1b** (8.5 mm), and c) **1a** + **1b** (8 mm each). The resonances were assigned to **1a** (○), (**1a**)₂ (●), **1b** (△), (**1b**)₂ (▲), and **1a**·**1b** (◆). The signal of the peripheral amide NH protons of **1a** within single or within double helices appears at higher field in the aromatic region.

proportions of these signals allow calculation of the dimerization constants as $K_{\text{dim}}(\mathbf{1a})_2 = 30 \text{ L mol}^{-1}$ ($\Delta G_{\text{dim}}(\mathbf{1a})_2 = -8.4 \text{ kJ mol}^{-1}$) and $K_{\text{dim}}(\mathbf{2a})_2 = 120 \text{ L mol}^{-1}$ ($\Delta G_{\text{dim}}(\mathbf{2a})_2 = -11.9 \text{ kJ mol}^{-1}$) in CDCl₃ at 25 °C—the difference between the two being assigned to effects of terminal substituents (decanoylamino versus *tert*-butylcarbamate) and side chains (decyloxy versus hydrogen). Recently, we showed that oligomers possessing 2,6-diaminopyridines as their terminal residues can be cleanly converted into the corresponding bis(pyridine *N*-oxide)s in the presence of *meta*-chloroperbenzoic acid (MCPBA), with only the terminal residues oxidized.^[13] Specifically, **1a** was converted into **1b** and pentamer **3a** into **3b**. Furthermore, the *N*-oxidized oligomers also possess the ability to hybridize into double-helical dimers:

[*] Dr. C. Zhan, Dr. I. Huc
 Institut Européen de Chimie et Biologie
 2 rue Robert Escarpit
 33607 Pessac (France)
 Fax: (+33) 540-00-22-15
 E-mail: i.huc@iecb.u-bordeaux.fr
 Prof. J.-M. Léger
 Laboratoire de Pharmacochimie
 146 rue Léo Saignat
 33076 Bordeaux (France)

[**] This work was supported by the CNRS, the University of Bordeaux I, the University of Bordeaux II, and by the French Ministry of Research and Education. We thank J. Lefeuvre for performing ab initio calculations.

Supporting information for this article is available on the WWW under <http://www.angewandte.org> or from the author.

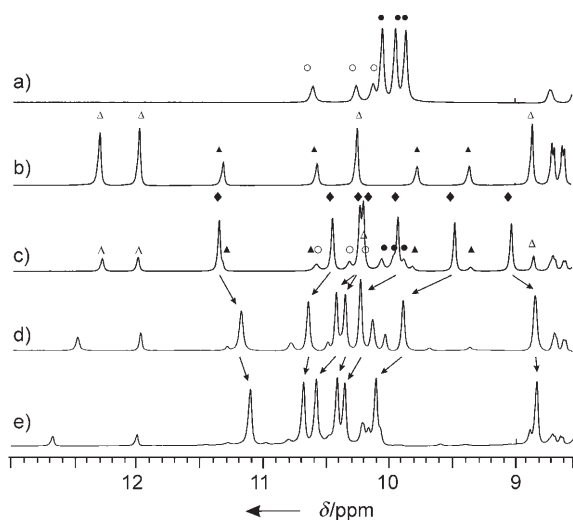


Figure 2. Partial 400 MHz ^1H NMR spectra showing the amide resonances of: a) **2a** at 25°C (32 mM), b) **2b** at 25°C (32 mM), c) **2a**+**2b** at 25°C (32 mM each), d) **2a**+**2b** at 0°C (32 mM each), and e) **2a**+**2b** at -25°C (32 mM each). The resonances were assigned to **2a** (○), (**2a**)₂ (●), **2b** (△), (**2b**)₂ (▲), and **2a-2b** (◆). The signal of the peripheral amide NH protons of **1a** within single or within double helices appears at higher field in the aromatic region.

spectra such as that shown in Figure 1b allow calculation of $K_{\text{dim}}(\mathbf{1b})_2 = 125 \text{ L mol}^{-1}$ ($\Delta G_{\text{dim}}(\mathbf{1b})_2 = -12.0 \text{ kJ mol}^{-1}$); this value is about four times higher than $K_{\text{dim}}(\mathbf{1a})_2$.^[13]

The AOA are amenable to chemical transformations but still retain their ability to hybridize, which prompted us to explore the possibility of cross-hybridization between chemically different oligomers. Thus when **1a** and its di-*N*-oxide **1b** are mixed in stoichiometric amounts (8 mM each), the NMR spectrum (Figure 1c) shows minor signals of both monomers and both homodimers, but the spectrum is dominated by new signals, the multiplicity of which exactly corresponds to that expected for heterodimer **1a-1b**. The variation in the intensities of these signals, which decrease upon diluting or heating the solution, and their low chemical shifts are consistent with this assignment. Most importantly, the cross-hybrid seems considerably more stable than either of the homodimers: $K_{\text{assoc}}(\mathbf{1a-1b}) = 1140 \text{ L mol}^{-1}$, which corresponds to $\Delta G_{\text{assoc}}(\mathbf{1a-1b}) = -17.4 \text{ kJ mol}^{-1}$. In the hypothetical case where each individual strand would bring the same stabilization energy to a duplex regardless of its nature, the expected value would have been $\Delta G_{\text{assoc}}(\mathbf{1a-1b}) = (\Delta G_{\text{dim}}(\mathbf{1a})_2 + \Delta G_{\text{dim}}(\mathbf{1b})_2)/2 - RT \ln(2) = -11.5 \text{ kJ mol}^{-1}$ (the second term accounts for the statistical factor that favors cross-hybridization at the expense of homodimerization). The heterodimer is thus stabilized by 5.9 kJ mol^{-1} relative to this theoretical value.

Oligomers **1a** and **1b** have long alkyl chains and do not crystallize. Unsubstituted heptamer **2a**, however, is highly crystalline and has been characterized in the solid state, both as a single helix and as a double helix.^[12] We thus prepared heptamer bis-*N*-oxide **2b** and heptamer mono-*N*-oxide **2c** from **2a** in the hope that crystals of the heterodimer could be grown. This proved unsuccessful and only single helical **2b** could be characterized (in several crystalline forms).^[20]

However, the behavior of **2a**, **2b**, and **2c** in solution is fully consistent with that of **1a** and **1b**. As shown in Figure 2b and c, bis-*N*-oxide dimerizes with $K_{\text{dim}}(\mathbf{2b})_2 = 22 \text{ L mol}^{-1}$ ($\Delta G_{\text{dim}}(\mathbf{2b})_2 = -7.6 \text{ kJ mol}^{-1}$)^[21] while **2a** and **2b** cross-hybridize with $K_{\text{assoc}}(\mathbf{2a-2b}) = 650 \text{ L mol}^{-1}$ ($\Delta G_{\text{assoc}}(\mathbf{2a-2b}) = -16.1 \text{ kJ mol}^{-1}$). The cross-hybrid is more stable by 5.1 kJ mol^{-1} relative to the theoretical value of $(\Delta G_{\text{dim}}(\mathbf{2a})_2 + \Delta G_{\text{dim}}(\mathbf{2b})_2)/2 - RT \ln(2) = -11.0 \text{ kJ mol}^{-1}$. Cross-hybrid **2a-2b** prevails at 25°C (Figure 2c) and even more so at lower temperatures (Figure 2d,e), although the other species then become too minor to determine the K_{assoc} values accurately.

Heptamer **2c**, which contains only one *N*-oxide function, can in principle form parallel and antiparallel dimers, depending on whether the *N*-oxide functions of the two strands reside at the same end or at opposite ends of the duplex. Figure 3

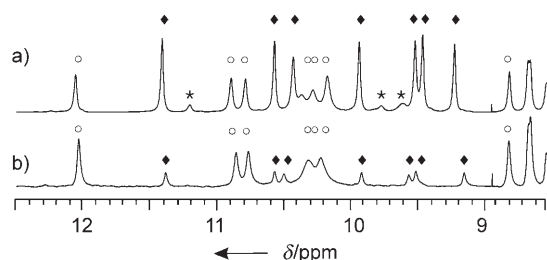


Figure 3. Partial 400 MHz ^1H NMR spectra at 25°C showing the amide resonances of **2c** at a) 32 mM and b) 2 mM. The resonances were assigned to **2c** (○), antiparallel (**2c**)₂ (◆), and parallel (**2c**)₂ (*). The signal of one of the two peripheral carbamate NH protons of **2c** appears at higher field in the aromatic region.

shows that two sets of signals can indeed be assigned to two different dimers, but that their amounts differ by a factor of 7.8, which represents an energy difference between the two dimers of $\Delta \Delta G_{\text{dim}}(\mathbf{2c}) = 5.1 \text{ kJ mol}^{-1}$. The NMR spectra alone do not allow an unambiguous assignment of the two sets of signals. However, it seems reasonable to assign the major species to antiparallel (**2c**)₂ and the minor species to parallel (**2c**)₂ on the basis of the stability of **1a-1b** and **2a-2b**, in which only one *N*-oxide function is found at each end of the duplex.

Complete solid-state characterization of the homo- and heterodimerization products was obtained with pentamers **3a** and **3b**. As shown in Figure 4, the homodimer was obtained when either **3a** or **3b** was left to crystallize alone,^[12,13] but cocrystals of the two strands (a heterodimer) were obtained when an equimolar mixture of the two was left to crystallize.^[22] The structure of **3a-3b** is remarkably similar to that of (**3b**)₂ (Figure 4) despite the fact that the unit cells, the space groups, and the crystallization solvent (and thus the included solvent molecules) of the two crystals are different. The relative positions of the two strands and the interactions between them (for example, aromatic...aromatic distances and a single interstrand NH...ON hydrogen bond) are identical in **3a-3b** and (**3b**)₂. These findings corroborate the solution studies and supports the complete compatibility between the hybridization of the two series of AOA. However, it does little to clarify the origin of the larger stability of heterodimers which presumably lies in electro-

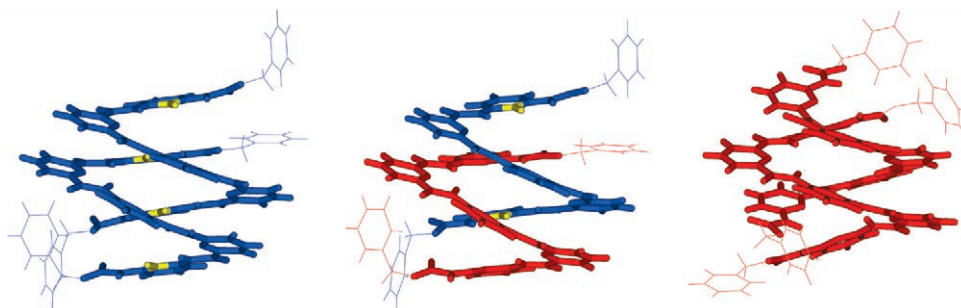


Figure 4. Stick representation of the crystal structures of **(3b)₂** (left), **3a-3b** (center), and **(3a)₂** (right). The *N*-oxide functions are shown in yellow. Included solvent molecules are omitted for clarity.

static interactions between amide, pyridine, and pyridine *N*-oxide moieties. Specifically, the surprising stack of four pyridine *N*-oxide rings with all their dipoles in a parallel orientation, as observed in the structure of **(3b)₂**, certainly causes unfavorable electrostatic interactions that are relieved in the structure of **3a-3b**. We performed ab initio density functional theory calculations (RHF, 6-31G* basis set) using GAMESS^[23] to evaluate the electrostatics of the pyridine and pyridine *N*-oxide molecules. The dipole moment of pyridine is estimated as 2.31 D, whilst that of pyridine *N*-oxide is more than twice as large (5.24 D) and has the same orientation. In addition to dipolar interactions, local charges certainly come into play. The partial charge on the pyridine nitrogen atom is -0.51 whilst that on the pyridine *N*-oxide nitrogen atom is only -0.07 , with the electrons being located on the oxygen atom (-0.62). One may actually wonder why the pyridine *N*-oxide oligomers hybridize at all. Orbital electron densities show that the π clouds of pyridine *N*-oxide are not as electron-rich as those of pyridine, which probably favors face-to-face π - π interactions with the *N*-oxides.

It is worth noting that each aromatic ring within the **3a-3b** duplex interacts directly with two other aromatic rings, one below and one above. The stability of a given duplex may thus be affected in a complex way, depending on whether the rings above and below each aromatic unit are oxidized or not. In DNA, base-pairing energy is known to vary significantly depending on the nature of the neighboring base pairs; such effects could be even more pronounced in heptameric or pentameric molecular duplexes such as **1a-1b** and **3a-3b**.

The tendency of *N*-oxide AOs to hybridize with their precursors rather than with themselves represents an original example of cross-hybridization. It contrasts with other experiments where self-recognition was reported to prevail over heterologous recognition.^[24] The hybridization of AOs may provide a means to elaborate complex sequence-selective hybridization of longer oligomers and more than two *N*-oxide functions per duplex.

Received: February 28, 2006
 Published online: June 21, 2006

Keywords: helical structures · molecular recognition · supramolecular chemistry

- [1] X. Li, D. R. Liu, *Angew. Chem.* **2005**, *116*, 4956; *Angew. Chem. Int. Ed.* **2004**, *43*, 4848; T. M. Snyder, D. R. Liu, *Angew. Chem.* **2005**, *117*, 7545; *Angew. Chem. Int. Ed.* **2005**, *44*, 7379.
 [2] N. C. Seeman, *Angew. Chem.* **1998**, *110*, 3408; *Angew. Chem. Int. Ed.* **1998**, *37*, 3220; P. W. K. Rothemund, A. Ekani-Nkodo, N. Papadakis, A. Kumar, D. K. Fygenon, E. Winfree, *J. Am. Chem. Soc.* **2004**, *126*, 16344; M. Endo, N. C. Seeman, T. Majima, *Angew. Chem.* **2005**, *117*, 6228; *Angew. Chem. Int. Ed.* **2005**, *44*, 6074; A. Y. Koyfman,

- G. Braun, S. Magonov, A. Chworos, N. O. Reich, L. Jaeger, *J. Am. Chem. Soc.* **2005**, *127*, 11886; S. H. Park, C. Pistol, S. J. Ahn, J. H. Reif, A. R. Lebeck, C. Dwyer, T. H. LaBean, *Angew. Chem.* **2006**, *118*, 749; *Angew. Chem. Int. Ed.* **2006**, *45*, 735;
 [3] M. Albrecht, *Angew. Chem.* **2005**, *117*, 6606; *Angew. Chem. Int. Ed.* **2005**, *44*, 6448.
 [4] X. Yang, B. Gong, *Angew. Chem.* **2005**, *117*, 1376; *Angew. Chem. Int. Ed.* **2005**, *44*, 1352.
 [5] M. Albrecht, *Chem. Rev.* **2001**, *101*, 3457; C. Piguet, G. Bernardinelli, G. Hopfgartner, *Chem. Rev.* **1997**, *97*, 2005.
 [6] E. A. Archer, M. J. Krische, *J. Am. Chem. Soc.* **2002**, *124*, 5074; H. Gong, M. J. Krische, *J. Am. Chem. Soc.* **2005**, *127*, 1719; E. A. Archer, A. E. Sochia, M. J. Krische, *Chem. Eur. J.* **2001**, *7*, 2059.
 [7] A. P. Bisson, F. J. Carver, D. S. Eggleston, R. C. Haltiwanger, C. A. Hunter, D. L. Livingstone, J. F. MacCabe, C. Rotger, A. E. Rowan, *J. Am. Chem. Soc.* **2000**, *122*, 8856.
 [8] B. Gong, Y. Yan, H. Zeng, E. Skrzypczak-Jankun, Y. Wah Kim, J. Zhu, H. Ickes, *J. Am. Chem. Soc.* **1999**, *121*, 5607; H. Zeng, R. S. Miller, R. A. Flowers II, B. Gong, *J. Am. Chem. Soc.* **2000**, *122*, 2635.
 [9] P. S. Corbin, S. C. Zimmerman, *J. Am. Chem. Soc.* **2000**, *122*, 3779; P. S. Corbin, S. C. Zimmerman, P. A. Thiessen, N. A. Hawryluk, T. J. Murray, *J. Am. Chem. Soc.* **2001**, *123*, 10475.
 [10] C. Schmuck, W. Wienand, *Angew. Chem.* **2001**, *113*, 4493; *Angew. Chem. Int. Ed.* **2001**, *40*, 4363; C. Schmuck, W. Wienand, *J. Am. Chem. Soc.* **2003**, *125*, 452.
 [11] B. Di Blasio, E. Benedetti, V. Pavone, C. Pedone, *Biopolymers* **1989**, *28*, 203.
 [12] V. Berl, I. Huc, R. Khoury, M. J. Krische, J.-M. Lehn, *Nature* **2000**, *407*, 720; V. Berl, I. Huc, R. Khoury, J.-M. Lehn, *Chem. Eur. J.* **2001**, *7*, 2810; V. Maurizot, J.-M. Léger, P. Guionneau, I. Huc, *Russ. Chem. Bull.* **2004**, *113*, 1572; H. Jiang, V. Maurizot, I. Huc, *Tetrahedron* **2004**, *60*, 10029.
 [13] C. Dolain, C. Zhan, J.-M. Léger, I. Huc, *J. Am. Chem. Soc.* **2005**, *127*, 2400.
 [14] B. Hasenknopf, J.-M. Lehn, G. Baum, D. Fenske, *Proc. Est. Acad. Sci. Eng. Proc. Natl. Acad. Sci. USA* **1996**, *93*, 1397; J.-M. Lehn, *Chem. Eur. J.* **2000**, *6*, 2097.
 [15] H. Zeng, H. Ickes, R. A. Flowers II, B. Gong, *J. Org. Chem.* **2001**, *66*, 3574.
 [16] Y. Tanaka, H. Katagiri, Y. Furusho, E. Yashima, *Angew. Chem.* **2005**, *117*, 3935; *Angew. Chem. Int. Ed.* **2005**, *44*, 3867.
 [17] G. J. Gabriel, B. L. Iverson, *J. Am. Chem. Soc.* **2002**, *124*, 15174; Q.-Z. Zhou, X.-K. Jiang, X.-B. Shao, G.-J. Chen, M.-X. Jia, Z.-T. Li, *Org. Lett.* **2003**, *5*, 1955.
 [18] V. Berl, I. Huc, R. Khoury, J.-M. Lehn, *Chem. Eur. J.* **2001**, *7*, 2798; I. Huc, V. Maurizot, H. Gornitzka, J.-M. Léger, *Chem. Commun.* **2002**, 578; C. Dolain, A. Grélard, M. Laguerre, H. Jiang, V. Maurizot, I. Huc, *Chem. Eur. J.* **2005**, *11*, 6135.
 [19] A. Acocella, A. Venturini, F. J. Zerbetto, *J. Am. Chem. Soc.* **2004**, *126*, 2362.

- [20] See the Supporting Information.
- [21] The presence of two *N*-oxide groups in **2a** slightly lowers its ability to hybridize whereas the contrary occurs for **1a**, thus suggesting that side-chain and terminal-group effects are complex and do not operate in the same manner on the oxidized oligomers as they do on their precursors.
- [22] Crystal data for **3a·3b**: C₁₀₈H₈₂N₃₀O₂₄·CHCl₃·C₃H₇NO·2H₂O, *M*_r = 2412.53, crystal size 0.10 × 0.10 × 0.05, monoclinic, space group *P*21/*n*, *Z* = 4, *a* = 26.0433(12), *b* = 14.5247(3), *c* = 26.6580(10) Å, β = 115.935(2), *V* = 9068.4(6) Å³, ρ_{calcd} = 1.767 mg m⁻³, *T* = 163(2) K, θ_{min} = 6.33, θ_{max} = 50.43, λ = 1.54180 Å. Radiation type Cu_{Kα}, μ(Cu_{Kα}) = 1.871 mm⁻¹. Data collected on a Rigaku MM007-Rapid R-Axis diffractometer with confocal optics. Of 95 321 reflections measured, 9455 were unique (*R*_{int} = 0.2080), 5092 with *I* > 2σ(*I*), 1271 parameters in the final refinement. The structure was solved by direct methods and refined by full-matrix least-squares on *F*² (SHELXL version 6.12). The final *R* indices were *R*₁ (*I* > 2σ(*I*)) = 0.1218, *wR*₂(*F*²) = 0.3439 (all data). CCDC-299505 contains the supplementary crystallographic data for this paper. These data can be obtained free of charge from The Cambridge Crystallographic Data Centre via www.ccdc.cam.ac.uk/data_request/cif.
- [23] M. W. Schmidt, K. K. Baldrige, J. A. Boatz, S. T. Elbert, M. S. Gordon, J. H. Jensen, S. Koseki, N. Matsunaga, K. A. Nguyen, S. J. Su, T. S. Windus, M. Dupuis, J. A. Montgomery, *J. Comput. Chem.* **1993**, *14*, 1347.
- [24] A. Wu, L. Isaacs, *J. Am. Chem. Soc.* **2003**, *125*, 4831; D. Bilgiçer, X. Xing, K. Kumar, *J. Am. Chem. Soc.* **2001**, *123*, 11 815.